

# **Smart Manufacturing and Material Processing** (SMMP)

DOI: http://doi.org/10.26480/smmp.01.2023.83.88





RESEARCH ARTICLE

# STRUCTURAL DESIGN AND ANALYSIS OF MINE FLAMEPROOF ELECTRIC ACTUATOR

Chuanzhi Songa,b,\*, Xueming Wanga,b, YU Qiua,b

- a Tiandi (changzhou) Automation Co., Ltd., Changzhou 213015, China
- b CCTEG Changzhou Research Institute, Changzhou 213015, China
- \*Corresponding Author Email: 354017556@qq.com

This is an open access article distributed under the Creative Commons Attribution License CC BY 4.0, which permits unrestricted use, distribution, and reproduction in any medium, provided the original work is properly cited.

#### **ARTICLE DETAILS**

# Article History:

Received 05 January 2024 Revised 08 February 2024 Accepted 11 March 2024 Available online 14 March 2024

#### **ABSTRACT**

According to the power supply environment in the coal mine and the operating requirements of the electric control of small diameter valves in the waterway network, the appropriate mechanical transmission structure of the mine electric actuator is designed, and the overall design and detailed transmission design are completed, Check the tooth surface contact strength and tooth root bending strength of the transmission gear. Through the analysis and strength check of the force on the gear shaft, meet the material requirements. Through the finite element analysis software, the hydrostatic pressure loading analysis of the flameproof shell is carried out. The calculated structural strength and stiffness meet the requirements, providing a theoretical basis for the reliable and stable operation of the mine flameproof electric actuator.

#### **KEYWORDS**

Small diameter valve, mine flameproof electric actuator, transmission design, strength check, finite element analysis

# 1. Introduction

Pipe network valve is an important control element of mine drainage pipe. The mine flameproof electric actuator is a commonly used driving device for the valve of coal mine pipe network. The pipeline valve stem is driven by the mine explosive electric actuator to realize the opening and closing of the pipeline valve. The mine flameproof electric actuator is mainly composed of motor, transmission mechanism, electrical parts, hand electric switching parts, shell parts, etc. The transmission mechanism and shell are the key components of the design of electric actuator, transmitting the input torque of the motor, so as to realize the opening and closing of the valve, the shell mainly plays the role of explosive protection, and is an important carrier of transmission mechanism and electronic components.

At present, domestic and foreign scholars have conducted a lot of research on the structure of electromechanical integration of electric actuators. Ding Shifeng designed an explosion-proof fine small valve electric actuator based on SolidWorks, which was driven by AC motor and combined with spur gear set and worm gear (Ding et al., 2020). Ma Chuanxin et al. [2] designed a high-efficiency, low-power high-torque electric actuator, which adopts a double-planet transmission design (Ma et al., 2023). A group researchers designed a hybrid transmission scheme with a two-stage 2K-H (NGW) planetary reducer as the main transmission mechanism, combined with a fixed shaft gear train and worm gear (Long and Zeng, 2023). Shen Wei analyzed the key points of attention in engineering design of electric actuator from the aspects of torque safety factor range, calculation and selection of gear box and selection of thrust conversion device based on application examples of engineering projects (Shen, 2019). Li Apeng designed a non-contact type flat scroll spring to meet the requirements of intelligent variable frequency electric actuator/hand switching (Li, 2022).

The electromechanical integration of the existing electric actuator is mainly studied from the transmission design and the design of the manual

automatic switching device. The output torque value designed is relatively large, which cannot meet the requirements of small caliber, small torque and small volume valve actuators. This paper designs a compact structure, stable and reliable transmission and easy assembly for the underground environment of coal mine. Mine flameproof electric actuator for small diameter valve, Design, check and calculate the transmission mechanism and manual switching device, and analyze and calculate the static pressure load of the flameproof shell to ensure the rationality and reliability of the transmission mechanism and shell structure, which has important engineering significance to ensure the safe operation of the flameproof electric actuator for small caliber mine in the coal mine.

### 2. Overall Design of Electric Actuator

Mine explosion-proof electric small-diameter valve is widely used in coal mine water treatment system, mine dust removal system, water pump automatic control system, coal mine underground cooling system, gas extraction system, jet grouting machine, working face water system and other systems. In view of the working requirements of low pressure, small caliber, partial rotary valve, and the power supply environment in the coal mine is relatively bad. The DC motor is used to drive, and after the deceleration device, the torque and speed meet the driving requirements. The output shaft of the deceleration device is connected with the valve stem to realize the opening and closing of the valve.

According to the use requirements, the service life of the mine flameproof electric actuator is at least two years, the valve is opened and closed twice a day, the output speed is about 1RPM, the output torque is 40Nm, the performance is stable and reliable, and the shell meets the explosion-proof requirements of the coal mine.

#### 2.1 Transmission Scheme Design

In order to meet the compact structure, select the relatively small DC motor, 12v power supply, the rated power is 15w, the rated output torque



Access this article online

Website:

We b site: www.topics on chemeng.org.my

**DOI:** 10.26480/smmp.01.2023.83.88

is 0.015 Nm, and the rated output speed is 5480 RPM.

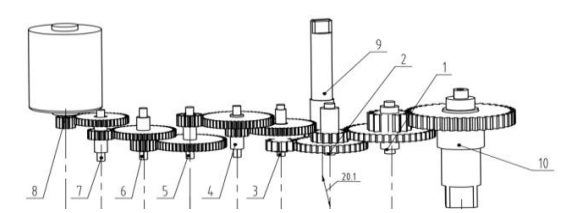
Due to the high speed and low torque of the DC motor, under the requirements of achieving the required output torque, output speed and service life, the transmission ratio needs to bear the balanced distribution of load capacity, and to meet the transmission strength.

For the design of the transmission scheme, the electric actuator generally adopts the following three ways or the combination way

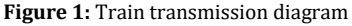
 Direct gear easy to process, simple structure, strong bearing capacity, but the transmission level stability is poor and easy to impact

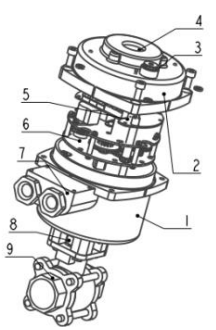
- Worm gear large transmission ratio, compact structure, smooth transmission, self-locking, but large heat rate, low efficiency.
- Planetary gear large bearing capacity, high efficiency, stable operation, but complex structure, manufacturing and installation is more troublesome.

In order to meet the requirements of compact structure and large transmission ratio, considering the demand for low output torque, the multi-stage straight gear combined transmission mode is adopted, as shown in Figure.1.



1-Gear shaft 1, 2-Gear shaft 2, 3-Gear shaft 3, 4-Gear shaft 4, 5-Gear shaft 5, 6-Gear shaft 6, 7-Gear shaft 7, 8-Motor shaft, 9-Manual shaft, 10-Spindle





1-Lower mining flameproof shell, 2-Upper mining flameproof shell, 3-Hand electric switching device, 4-Observation window, 5-Control circuit board, 6-Reducer, 7-Outlet nozzle, 8-Drive shaft, 9-Small diameter valve

Figure 2: Structure diagram of mine electric actuator

In the national standard "GB / T 24923-2010 Technical Conditions of General Valve Electric Device", it is stipulated that the manual mechanism can be divided into hand electric switching mechanism and manual operation mechanism (the operation mechanism is the hand wheel and hand wheel shaft), which is used for manually operating the valve stem rotation, and the function of the switching mechanism is to realize the conversion between electric operation and manual operation (Shen, 2019). In the case of power failure, the valve can be manually opened and closed, using the use of semi-automatic electric switching form. The manual shaft is engaged directly with the large gear of gear shaft 2, and during the manual operation, the motor power off and rotate the manual shaft to drive the main shaft. The observation window and hand automatic switch device are set on the upper mining flameproof shell, and two outlet nozzle are set on the side of the lower mining flameproof shell. Four screws are fixed between the upper mining flameproof shell and the lower mining flameproof shell, the small diameter valve is fixed at the bottom of the

lower mining flameproof shell, and the protruding shaft of the reducer box is connected with the small diameter valve through the drive shaft, as shown in Figure.2.

#### 2.2 Gear Design

From the motor output shaft speed, the total transmission ratio is about 5480, the pressure angle of gear transmission is  $20^\circ$ , adopt small module gear, choose 0.5, 0.8 and 1 respectively, and the transmission efficiency of straight gear is 0.95. According to the design specification of gear, to meet the stability and bearing capacity of gear transmission, the coincidence degree should be greater than the allowable value of 1.4, through the gear parameters, the spatial position of the deceleration mechanism and the output torque and speed, the manual shaft gear mesh with the large gear of the gear shaft 2, and the number of teeth is designed as 15. The main parameters of electric drive are shown in Table 1.

Table 1: Main parameters of straight tooth transmission (electric)										
	gear shaft	number of teeth Z	breadth of tooth b/mm	centre-to- centre spacing a/mm	contact ratio and overlap ratio ε	speed n/rpm	torsion T/Nm	radial force Fr/N		
Level 1	motor shaft	13	5	13.5 16.25	1.58 1.64	5480	0.015	0.02		
	Gear shaft 7	41	3			1738	0.045			
Level 2		18	4					0.07		
	Gear shaft 6	47	3			665.4	0.11			
Level 3		18	7	- 18	1.65			0.18		
Level 5	Gear shaft 5	54	4			221.8	0.3			
Level 4		18	5	18.25	1.65			0.52		
Level 4	Gear shaft 4	55	4			72.6	0.9			
Level 5		16	5	17	1.63			1.34		
Level 5	Gear shaft 3	52	3			22.3	2.8			
Lovel 6	Geal Shart 5	12	4	18.9	1.49	44.3	2.0	4.97		
Level 6	Gear shaft 2	35	3			7.65	7.9			
Level 7		16	4	23.2	1.61			18.38		
	Gear shaft 1	42	3			2.9	19.7			
Level 8	Gear Shart 1	15	7	27.5	1.6	2.9	17./	53.71		
	principal axis	40	6			1.09	49.8			

After calculation, as shown in Table 1, the output torque of the spindle is 1.24 times of the required torque, which meets the torque output requirements, the spindle output speed is slightly greater than the required speed, which meets the requirements of valve operation.

#### 2.2.1 Gear strength Check

By calculating the safety factor  $s_H$  of the contact stress  $\sigma_H$  and allowable contact stress  $\sigma_{HP}$  between gears, judge whether the contact strength of the gear meets the requirement.

By calculating the safety factor of the ratio between the bending stress of the tooth root  $\sigma_F$  and the allowable bending stress of the tooth root  $\sigma_{FP}$  when the gear meshes, the bending strength of the tooth root meets the requirements (Li, 2022; Nguyen, 2023; Koutsoupakis et al., 2023; Donmez and Kahraman, 2023; Muzzioli et al., 2022).

1) Check the contact strength of the gear and tooth surface

The calculation formula of contact stress of external gear is

$$\sigma_{H} = Z_{H}Z_{E}Z_{\xi} Z_{\beta} \sqrt{\frac{2F_{t}}{db} \frac{u+1}{u}} \sqrt{K_{A}K_{V}K_{H\alpha}K_{H\beta}} \tag{1}$$

Formula-

K<sub>A</sub>-Coincidence coefficient,

K<sub>V</sub>-Gear engagement coefficient,

 $K_{H\alpha}$ -Coefficient of load distribution between teeth,

KHB-Tooth load distribution coefficient

Z<sub>H</sub>-Node area coefficient

Z<sub>E</sub>-Single pair tooth engagement coefficient

 $Z_{\epsilon}$ -Coefficient of coincidence

 $Z_{\beta}$ -Single pair tooth engagement coefficient

# 2.3 Gear Shaft Design and Check

d-Separation circle diameter, mm,

b-Tooth width, mm,

m-modulus,

Ft-Circular force generated by gear engagement, N,

u--Drive ratio.

The calculation formula for the allowable contact stress is

$$\sigma_{HP} = \frac{Z_{NT} \sigma_{Hlim}}{S_{Hmin}} \tag{2}$$

 $Z_{NT}\text{-}Formula\text{-}life\,\, coefficient,}\,\,\, \sigma_{Hlim}\text{-}test\,\, gear\,\, fatigue\,\, limit,}\,\,\, MPa,\, S_{Hmin}\,\, \text{-}minimum\,\, safety\,\, factor,}$ 

After calculation, all engaged gear safety factor is> 1, and the contact strength of gear tooth surface meets the transmission requirements.

2) Check the bending strength of the gear root

The formula for calculating the root bending stress is

$$\sigma_{F} = \frac{F_{t}}{hm} K_{A} K_{V} K_{H\alpha} K_{H\beta} Y_{F} Y_{S} Y_{\epsilon} Y_{\beta} Y_{B}$$
(3)

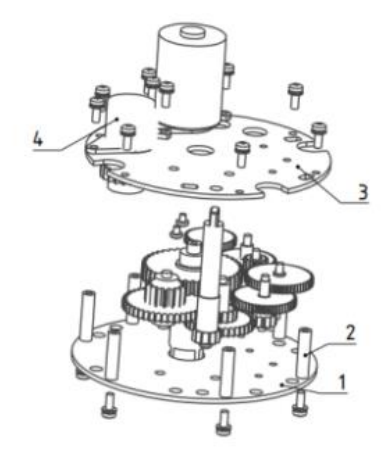
 $Y_F$  is Tooth shape coefficient,  $Y_S$  is Stress correction coefficient,  $Y_E$  is Coincidence coefficient,  $Y_B$  is Spiral angle coefficient,  $Y_B$  is Rim coefficient.

The calculation formula of the allowable tooth root bending stress is

$$\sigma_{\rm FP} = \frac{\sigma_{\rm Flim} Y_{\rm ST} Y_{\rm N} Y_{\rm D} Y_{\rm R} Y_{\rm X}}{S_{\rm Uprin}} \tag{4}$$

 $Y_{ST}$  is Correction coefficient,  $Y_{N}$  is Calculated life coefficient,  $Y_{D}$  is Root fillet sensitivity coefficient,  $Y_{R}$ -Root surface condition coefficient,  $Y_{X}$  is Dimension coefficient,  $\sigma_{Flim}$  is Bending fatigue limit, MPa,  $S_{Hmin}$  is Minimum safety factor,

After calculation, all engaged gear safety factor > 1, and the contact strength of gear tooth surface meets the transmission requirements.



1-Lower cover plate, 2-mounting column, 3-upper cover plate, 4-Encoder assembly

Figure 3: Schematic diagram of the reducer box structure

As shown in Figure 3, multiple mounting columns are fixed on the upper and lower cover plates, and the gears at all levels are reasonably arranged, so that all gears can fully engage and avoid interference, and transmit torque stably and reliably, and read the position of the output shaft through the encoder assembly. Design the length of the gear shaft according to the thickness of the gear and the position of the double gear

on the gear shaft, correct the gear shaft diameter according to the torque received at each level. From the force of gear shaft, all levels of gear shaft can be divided into two categories cantilever beam and simple support beam. Motor shaft simplify cantilever shaft, manual shaft and output shaft, double gear simplify the calculation and analysis of simple support beam.

1) Force analysis of the motor shaft



Figure 4: Force diagram of motor shaft

As shown in Figure.4, find the support reverse force, then solve the shear force equation of the axis, expression

$$F_{S}(x) = \begin{cases} F_{r} l & (0 < x < a) \\ 0 & (a \le x < l) \end{cases}$$
 (5)

Solve the bending moment equation of the axis, the expression

$$M(x) = \begin{cases} F_{r1}x & (0 < x < a) \\ 0 & (a \le x < l) \end{cases}$$
 (6)

Judging from the moment diagram, the maximum moment is at the section cantilever, and  $Mmax = F_{r1}a$ 

#### 2) Force analysis of double coupling gear shaft

Double gear, output shaft and manual shaft are all in the form of simple support beam, with double gear as the analysis and calculation object. The double coupling gear shaft is simplified according to the engagement situation, as shown in Figure 5.

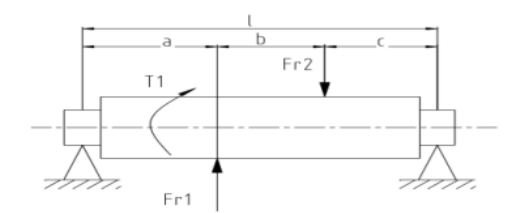
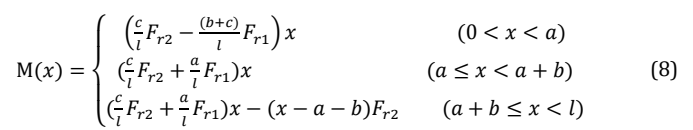


Figure 5: Simplified force diagram of double coupling gear shaft

From the equilibrium equation  $\Sigma F=0$ ,  $\Sigma M_A=0$ , Find the support reverse force, then solve the shear force equation of the axis, expression

$$F_{S}(x) = \begin{cases} \frac{c}{l} F_{r_{2}} - \frac{(b+c)}{l} F_{r_{1}} & (0 < x < a) \\ \frac{c}{l} F_{r_{2}} + \frac{a}{l} F_{r_{1}} & (a \le x < a + b) \\ \frac{c}{l} F_{r_{2}} - \frac{a}{l} F_{r_{1}} & (a + b \le x < l) \end{cases}$$
(7)

Solve the bending moment equation of the axis, the expression



From the moment diagram, the maximum moment is at section a+b, and Mmax =  $(\frac{c}{l}F_{r2}+\frac{a}{l}F_{r1})(a+b)$ 

Torque calculation and analysis

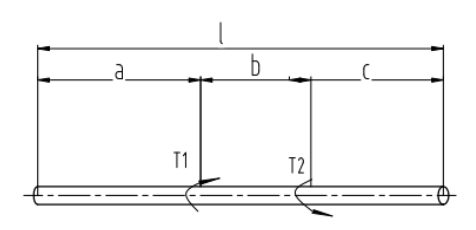


Figure 6: Torque by force drawing

As shown in Figure.6, from the equilibrium equation

$$T_1 + T_2 = 0$$
 (9)

$$T_1 = -T_2 = F_t d/2 \tag{10}$$

 $F_t$ —— Circumferential force generated by gear engagement, N,

*d*—— Scale circle, mm.

3) Check the deformation strength of the bending and torsion combination

According to the torque and bending moment diagram, it can be known that the torque and bending torque at the pinion mesh section is the maximum, which is the danger point.

Check against the strength conditions of the third strength theory

$$\frac{1}{w}\sqrt{Mmax^2 + {T_2}^2} \le [\sigma] \tag{11}$$

Where W — bending section coefficient W =  $\frac{\pi d^3}{32}$ , mm<sup>3</sup>.

4) The gear shaft material is 40 Cr, the surface quenching after modulation, strength limit  $\sigma_s{=}500 MPa$ , the hardness of tooth core is 220-250 HBS, and the tooth surface hardness reaches 50 HRc, bring the parameters of each gear shaft into the above equation for calculation. After calculation and checking, all gear shafts meet the strength requirements.

After theoretical calculation and check analysis, all levels of gear and gear shaft can meet the requirements.

# 3. HYDROSTATIC WATER PRESSURE ANALYSIS OF MINE ELECTRIC ACTUATOR SHELL

The shell of the mine electric actuator has the function of explosion isolation and protection, the shell is made of cast iron pouring, the shell is circular and 0-ring, the electric actuator drives the motor through the control circuit board, the reducer and the valve transmit torque through the transmission shaft, according to the overvoltage test (static pressure method) in GB/T3836.2-2021, and the internal volume of the shell is> $10\text{cm}^3$ , 1MPa, pressurization time for at least 10s, no structural damage or leakage through the shell wall, then pass the overpressure test (Gericke et al., 2023; Qinghua et al., 2021; Minghao et al., 2022; Zhiyuan et al., 2022). Therefore, the simulated hydrostatic pressure simulation analysis is conducted on the explosive isolation shell.

#### 3.1 Geometric Model Processing

The 3 D software is used to model the upper and lower mining flameproof shell. In order to improve the force analysis and calculation speed of the model, the upper and lower mining flameproof shell are simplified in the modeling process, and the influence of casting rounded corners on the overall performance is ignored. The geometric model is imported into the finite element analysis software, and the material properties of the mining flameproof shell are defined in the simulation software, as shown in Table 2

Table 2: Shell Material properties									
	modulus of elasticity /GPa	Poisson ratio	density/g/cm³	yield strength /MPa					
upper mining flameproof shell	169	0.275	7.1	>=250					
lower mining flameproof shell	169	0.275	7.1	>=250					

#### 3.2 Grid Division

To grid the model, the calculation time, accuracy and grid quality should be

considered. The overall grid size is 0.8mm, the number of grids is 468887, the number of nodes is 715980, and the average quality is 0.84, as shown in Figure 7.



Figure 7: Mesh division drawing

#### 3.3 Boundary Conditions Are Loaded

The contact between the upper and lower shells is defined as bonded contact. 1MPa hydrostatic pressure is applied to the shell for 13s, as shown in Figure.8, fixed constraints are set at the bottom of the lower shell, as shown in Figure 9.

# 3.4 The Strength and stiffness Calibration Criteria

For strength, because the shell parts is plastic material, the allowable stress is

$$[\sigma] = \frac{\sigma_s}{n_s}$$

 $\sigma_s$  - -Material yield limit

 $n_{\scriptscriptstyle S}$  - -Safety factor, the value taken in this paper is 1.5.

The allowable stress  $[\sigma]$  is calculated to be 166.7MPa.

For stiffness, the shell produces deformation displacement less than 1mm.

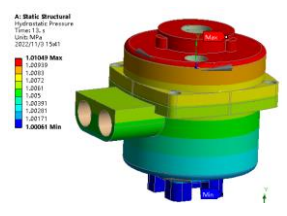


Figure 8: Hydrostatic load application drawing



Figure 9: Load constraint applied Fig

## 3.5 Analysis of the Simulation Calculation Results

The stress distribution of the calculated model, The maximum stress value of the upper and lower mining flameproof shell is 128.51 MPa, Located at the bottom of the lower explosive shell, The maximum stress value is lower than the allowable stress value of the material  $[\sigma]$ , Meet the strength requirements, As shown in Figure.10 and Figure.11, the overall maximum deformation displacement of the shell is 0.07 mm, Located on the upper part of the upper explosive shell, Small maximum deformation displacement, less than 1 mm, meet the stiffness requirements , As shown in Figure Figure.12 (a), the maximum stress of the lower shell is located at the lower edge of the shell, To be the maximum stress position of the entire mining flameproof shell, The maximum stress value is 128.51 MPa, As

shown in Figure Figure.12 (b), the maximum stress of the upper diaphragm shell is located at the junction between the observation window and the shell body. The maximum stress value is 46.19MPa. As shown in Figure.13 (a), the maximum deformation displacement of the lower diaphragm shell is 0.06mm, and located on the outside position of the outlet mouth of the lower shell , As shown in Figure.13 (b), the maximum deformation of the upper shell is 0.07mm, and located at the end of the observation window, position the manual shaft hole in the upper housing.

In conclusion, through calculation and analysis, the whole mining flameproof shell can meet the requirements of overpressure test under 1MPa hydrostatic pressure, and has a certain safety margin to meet the requirements of use.

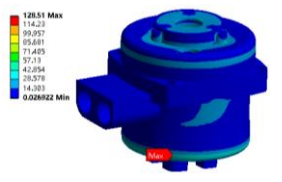


Figure 10: Stress cloud diagram of the upper and lower mining flameproof shell

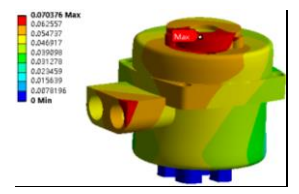
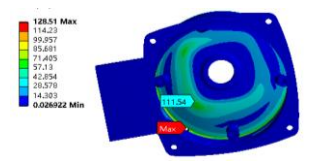
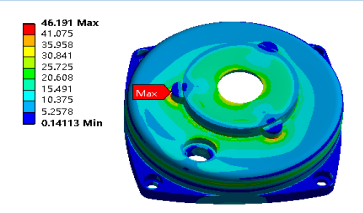


Figure 11: Upper and lower explosion shell, deformation and displacement cloud diagram

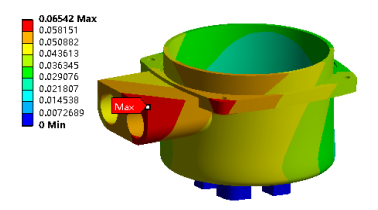


(a) Lower partition mining flameproof shell

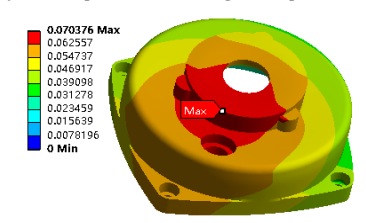


(b) Upper mining flameproof shell

Figure 12: stress cloud diagram of upper and lower mining flameproof shell



(a) Lower partition mining flameproof shell



(b) Upper mining flameproof shell

Figure 13: Deformation and displacement cloud diagram of the upper and lower mining flameproof shell

### 4. CONCLUSION

Based on the working environment of underground coal mine and the working characteristics of pipeline small diameter valve, select the DC motor drive, adopt multistage straight gear drive, design the contact strength of the gear surface and the bending strength of the tooth root, calculate the drive shaft, and calculate to meet the strength requirements. Through the finite element analysis software on the explosive shell through the hydrostatic water load analysis, calculate the maximum stress and maximum deformation value and position, and check the material strength, to ensure the transmission mechanism and the rationality of the shell structure and reliability, to ensure the safe operation of small diameter mine explosive electric actuator has important engineering significance.

#### **ACKNOWLEDGEMENT**

We gratefully acknowledge the financial support from the fund project: XZ202301ZY0002G based on ore -flow -based non -coal intelligent mines research (2023 Tibet Autonomous Region Science and Technology Key R & D Plan).

#### REFERENCES

- Ding, S., Li, Q., Huang, Y., 2020. Design of explosion-proof fine small valve electric actuator based on SolidWorks. Automation in Manufacturing Industry, 42 (07), Pp. 165-168.
- Donmez, A., Kahraman, A., 2023. An experimental and theoretical investigation of the influence of backlash on gear train vibro-impacts and rattle noise. Proceedings of the Institution of Mechanical Engineers, Part K: Journal of Multi-body Dynamics, 237 (1), Pp. 131-141.
- Gericke, P.B., Gericke, B.L., Teleguz, A.S., 2023. Evaluation of the degradation parameters of the technical state of mining machines with the use of the developed software. Mining equipment and electromechanics, 166 (02).
- Koutsoupakis, J., Seventekidis, P., Giagopoulos, D., 2023. Machine learning based condition monitoring for gear transmission systems using

- data generated by optimal multibody dynamics models. Mechanical Systems and Signal Processing. Pp. 190.
- Li, A., 2022. Design of planar Volute Spring for intelligent Variable frequency electric Actuator. Industrial Instrumentation and Automation Equipment, 285 (03), Pp. 46-48.
- Long, H., Zeng, X., 2023. Optimal Design of Planetary Reducer of Electric Actuator base on NSGA-II. Journal of Physics: Conference Series, 2492, (01).
- Ma, C., Chen, B., Chen, Y., 2023. Structure Design and Experimental Study of Double Planet Electric Actuator. Coal Mine Machinery, 44 (04), Pp. 16-18.
- Minghao, L., Hao, N., Jiayi, F., 2022. Optimization of coal loading performance of spiral drum of shearer. Journal of Mine Automation, 48 (10), Pp. 129-135.
- Muzzioli, G., Paini, G., Denti, F., 2022. A lumped parameter and CFD combined approach for the lubrication analysis of a helical gear transmission. Proceedings of the Institution of Mechanical Engineers Part D Journal of Automobile Engineering, 2385 (1).
- Nguyen, V.L., 2023. Design of an adjustable constant-force mechanism using a geared Sarrus linkage and spring. Mechanism and Machine Theory. Pp. 189.
- Qinghua, M., Yongqiang, Z., Xiaoyong, Z., 2021. Fault diagnosis of planetary gear transmission system of coal mining machines under variable speed working conditions. Journal of Mine Automation, 47 (07), Pp. 8-13.
- Shen, W., 2019. Discussion on Calculation and Selection of Electric Actuator of Valve. Chemical and Pharmaceutical Engineering, 40 (05), Pp. 47-52.
- Zhiyuan, S., Hu, T., Chi, M., 2022. Based on information fusion and convolution planetary gear box fault diagnosis of neural network. Journal of Mine Automation, 48 (9), Pp. 56-62.

